A DISCUSSION OF HYPERBOLICITY IN CATHENA 4: VIRTUAL MASS AND PHASE-TO-INTERFACE PRESSURE DIFFERENCES

N.U. Aydemir
Atomic Energy of Canada Limited, Chalk River, Ontario, Canada
aydemirn@aecl.ca

Abstract

It is well known that the one-dimensional equations of motion for two-phase flow are non-hyperbolic. Non-hyperbolicity can lead to numerical instabilities, destroying the solution. However, researchers in the last few decades were able to show that inclusion of virtual mass and/or phase-to-interface pressure differences in the momentum equations successfully render the equations of motion hyperbolic. In the present paper, the effect of including virtual mass and phase-to-interface pressure terms in the momentum equations on the hyperbolicity of the two-phase model in the CATHENA 4 code is discussed. The study is motivated by the fact that the inclusion of either model has been shown in the open literature to lead to a hyperbolic system separately. However, no known study exists that examine hyperbolicity in the presence of both these terms in the momentum equations. In this work, both terms are considered in the model equations simultaneously and their implications on the hyperbolicity of the two-phase model are discussed. Specifically, it is shown that in the case of mixed flow, there is a distinct region of non-hyperbolicity that developers need to be aware of when their equations include both the virtual mass and the phase-to-interface terms. Selecting the coefficients of phase-to-interface pressure difference terms properly ensures that the equations are hyperbolic for a wide range of conditions.

1. Introduction

CATHENA [1] is the primary thermalhydraulic network analysis tool used by Atomic Energy of Canada Ltd. (AECL) in the design, safety and licensing analysis of power and research reactors as well as test facilities.

A new version of the code, CATHENA 4 is currently under active development [2]. Although CATHENA 4 will inherit many of the hydraulic closure laws and heat transfer correlations from CATHENA 3, there are also significant changes in the numerical integration scheme, two-phase model, range of application, and language platform. For example, it is planned that the code will support three-field (continuous vapor, continuous liquid, entrained liquid), two-phase flow equations as opposed to the present version, which is based on a two-field model.

On the numerical front, the new code integrates the full non-linear set of two-phase field equations. This ensures that mass, energy, and momentum errors resulting from finite time discretization are identically zero. Errors resulting from out-of-range variables are corrected by standard means, that is, they are added back to the originating field. The field equations are cast in the Jacobian form and solved iteratively using Newton's method over the entire network.

The form of the momentum equations for one-dimensional two-phase flow is an important factor in the determination of the stability of the corresponding numerical scheme that is used to integrate them. The averaging operators that are applied to obtain the one-dimensional form inevitably result in loss of finer details of the flow field. Two such important phenomena are the virtual mass and the phase-to-interface pressure difference terms.

The virtual mass term is an interphase exchange term in the momentum equations and most relevant in the bubbly flow regime region. The traction at the interface depends on the geometry of the interface and the details of the flow field inside and outside of the bubble. However, such details of motion are lost during the averaging process. Drew et al. [3] has suggested that the virtual form should be proportional to an appropriate acceleration and derived an objective form based on principles of frame invariance. This form was expressed in terms of a single parameter and the relative acceleration of the phases. It forms the basis of the present paper as far as the effect of virtual mass on hyperbolicity is concerned. The general form for the virtual mass term suggested by Drew has been the subject of a number of subsequent investigations. For example, Watanabe et al. [4,5] has shown that using the objective form of the virtual mass with the proper choice of the virtual mass coefficient, leads to a hyperbolic system.

The second term in the momentum equations that can potentially affect the hyperbolicity of the field equations is the phase-to-interface pressure differences. This is discussed in detail by Stuhmiller [6], who proposed an additional term to be added to the momentum equation from first principles.

In Section 2, the field equations are given in their simplified form, that is, for a two-field model. Multifield equations of motion for CATHENA 4 can be found in [2].

In Section 3, the characteristic determinant of the system of equations is presented. The characteristic determinant includes terms arising from the inclusion of virtual mass as well as the phase-to-interface pressure terms. Section 3 also examines the conditions of hyperbolicity for a range of conditions in terms of the phase density ratios. These relations are given in the form of various inequalities that must be satisfied for the equations to remain in the hyperbolic region.

2. Field Equations

The multi-field equations for the one-dimensional two-phase model used in CATHENA 4 are given in their most general form in [2]. To simplify the analysis, the more often used form for two-fields is given. In this form, the governing equations for the two-fluid model consist of six conservation equations, that is, mass, momentum, and energy for each phase. Furthermore, the energy equations are of no interest in this paper since the characteristic velocities of the energy equation can be shown to be the same as convective velocities. Thus, only the mass and momentum equations will be considered in the current analysis. The mass and momentum equations are given by, Mass conservation, phase k

$$\frac{\partial}{\partial t}\left(\alpha_k\rho_k\right)+\frac{\partial}{\partial z}\left(\alpha_k\rho_k v_k\right)=m_{ki} \tag{1}$$

where, α_k, ρ_k, v_k are the phase volume fraction, density, velocity respectively and m_{ki} is the volumetric interface mass transfer rate.

Momentum Balance, phase k

$$\frac{\partial}{\partial t}\left(\alpha_k\rho_k v_k\right)+\frac{\partial}{\partial z}\left(\alpha_k\rho_k v_k v_k\right)+\alpha_k\frac{\partial P_k}{\partial z}+\beta_k\frac{\partial \alpha_k}{\partial z}=\tau_{kw}+\tau_{ki}+m_{ki}v_i-\alpha_k\rho_k g_z+(-1)^k M_{vm} \tag{2}$$

where P_k, τ_{kw}, τ_{ki} and g_z are the phase pressure, phase-to-wall friction, interface friction and acceleration due to gravity. The virtual mass term M_{vm} is given by

$$M_{vm}=\alpha_g\rho_f C_{vm}a_{vm} \tag{3}$$

In Equation (3), C_{vm} and a_{vm} are the virtual mass coefficient and the virtual mass acceleration, respectively. The latter is given in objective form by the expression [3],

$$a_{vm}=\frac{\partial(v_g-v_f)}{\partial t}+v_g\frac{\partial(v_g-v_f)}{\partial z}+\left[(\lambda-2)(v_g-v_f)\frac{\partial v_g}{\partial z}+(1-\lambda)(v_g-v_f)\frac{\partial v_f}{\partial x}\right] \tag{4}$$

Following [4, 5], in the present work λ has been chosen to be 2 so as to obtain agreement between analytical and experimental speeds of sound in two-phase flow.

In the characteristic analysis provided by [4], a simple, one-pressure model was assumed. As a result, the analysis of Watanabe excluded the affects of phase-to-interface pressure difference terms. In the present work, these terms will be referred to as the “beta” terms, referring to the term $\beta_k\frac{\partial \alpha_k}{\partial z}$ in Equation (2). The beta terms are defined in the following section.

3. Analysis of the Characteristics

CATHENA one-dimensional field equations can be arranged in the general form:

$$\mathbf{A}\frac{\partial \mathbf{U}}{\partial t}+\mathbf{B}\frac{\partial \mathbf{U}}{\partial z}=\mathbf{C} \tag{5}$$

along with the initial condition

$$\mathbf{U}(0,z)=\mathbf{G}(z) \tag{6}$$

represent a well-posed initial value problem if and only if the system of first order partial differential equations possesses real characteristics. System vector $\mathbf{U}$ is defined such that it has the components $P, \alpha_g, h_g, h_f, v_g, v_f$, where each components is a function time, and distance. The phase enthalpies, h_g and h_f are associated with the gas and liquid energy equations. The characteristics (or eigenvalues), μ, of the system given by Equation (5) can be determined from the sixth order polynomial,

$$\det(\mathbf{A}\mu - \mathbf{B}) = 0 \tag{7}$$

Since the characteristic speeds associated with the energy equations are simply v_g and v_f, the energy equations are not considered and the solution vector is reduced to P, α_g, v_g, v_f . Thus only four equations need to be considered in the present characteristic analysis.

The mass conservation equations are:

$$\rho_g \frac{\partial \alpha_g}{\partial t} + \frac{\alpha_g}{a_g^2}\frac{\partial P}{\partial t} + \frac{\alpha_g v_g}{a_g^2}\frac{\partial P}{\partial z} + \rho_g v_g \frac{\partial \alpha_g}{\partial z} + \alpha_g \rho_g \frac{\partial v_g}{\partial z} = \mathrm{m}_{gi} \tag{8}$$

$$\rho_f \frac{\partial \alpha_f}{\partial t} + \frac{\alpha_f}{a_f^2}\frac{\partial P}{\partial t} + \frac{\alpha_f v_f}{a_f^2}\frac{\partial P}{\partial z} + \rho_f v_f \frac{\partial \alpha_f}{\partial z} + \alpha_f \rho_f \frac{\partial v_f}{\partial z} = -\mathrm{m}_{gi} \tag{9}$$

where,

$$a_g^2 = \left(\frac{\partial \rho_g}{\partial P}\right)^{-1} \tag{10}$$

$$a_f^2 = \left(\frac{\partial \rho_f}{\partial P}\right)^{-1} \tag{11}$$

are the sound speed for gas and liquid phases, respectively. The gas and liquid mass conservation equations above are multiplied by v_g and v_f and subtracted from the corresponding momentum balance equations to obtain,

$$\alpha_g \rho_g \frac{\partial v_g}{\partial t} + \alpha_g \rho_g v_g \frac{\partial v_g}{\partial z} + \beta_g \frac{\partial \alpha_g}{\partial z} + \alpha_g \frac{\partial P}{\partial z} = -M_{vm} + \Phi_g \tag{12}$$

$$\alpha_f \rho_f \frac{\partial v_f}{\partial t} + \alpha_f \rho_f v_f \frac{\partial v_f}{\partial z} + \beta_f \frac{\partial \alpha_f}{\partial z} + \alpha_f \frac{\partial P}{\partial z} = M_{vm} + \Phi_f \tag{13}$$

where Φ_g and Φ_f denote the remaining non-derivative interface mass transfer, friction (wall and interface), and the gravity terms that do not affect the hyperbolicity of the system of equations. This is because the characteristic speeds are related to the wave propagation properties of the model and involve only the differential terms. The phase to interface pressure difference terms are given by the β_g and β_f terms where,

$$\beta_g = P_g - P_i \qquad \text{and} \qquad \beta_f = P_f - P_i \tag{14}$$

Proceeding with the characteristic analysis of the system given in Equations (8), (9), (12) and (13) a fourth order polynomial is obtained. However, considerable simplification can be achieved and the eigenvalue problem can be reduced to the solution of a second degree polynomial if the system of equations is re-arranged slightly. This involves rearranging the momentum equations as described below.

Adding the gas and momentum equations, the derivatives of the virtual mass term from one of the equations can be eliminated as follows:

$$\alpha_g \rho_g \frac{\partial v_g}{\partial t} + \alpha_f \rho_f \frac{\partial v_f}{\partial t} + \alpha_g \rho_g v_g \frac{\partial v_g}{\partial t} + \alpha_f \rho_f v_f \frac{\partial v_f}{\partial z} + (\beta_g - \beta_f) \frac{\partial \alpha_g}{\partial z} + \frac{\partial P}{\partial z} = 0 \tag{15}$$

Next, multiplying the gas momentum equation by α_f and the liquid momentum equation by α_g and subtracting them, the pressure term can be eliminated:

$$\begin{aligned} &\alpha_g \;\; \alpha_f \rho_g + \rho_f C_{vm} \;\; \frac{\partial v_g}{\partial t} - \alpha_g \;\; \alpha_f \rho_f + \rho_f C_{vm} \;\; \frac{\partial v_f}{\partial t} + \\ &\left[\alpha_f \alpha_g \rho_g + \alpha_g \rho_f C_{vm}(\lambda - 1)\right] v_g - \alpha_g \rho_f C_{vm}(\lambda - 2) v_f \;\; \frac{\partial v_g}{\partial z} - \\ &\left[\alpha_f \alpha_g \rho_f + \alpha_g \rho_f C_{vm}(1 - \lambda)\right] v_f - \alpha_g \rho_f C_{vm} \lambda v_g \;\; \frac{\partial v_f}{\partial z} + \;\; \alpha_f \beta_g + \alpha_g \beta_f \;\; \frac{\partial \alpha_g}{\partial z} = 0 \end{aligned} \tag{16}$$

The final system of equations is then given by Equations (8), (9), (15), and (16). This leads to the matrices $\mathbf{A}$ and $\mathbf{B}$ in the characteristic polynomial given in Equation (7) as follows:

$$\mathrm{A} = \begin{pmatrix} \dfrac{\alpha_g}{a_g^2} & \rho_g & 0 & 0 \\ \dfrac{\alpha_f}{a_f^2} & -\rho_f & 0 & 0 \\ 0 & 0 & \alpha_g \rho_g & \alpha_f \rho_f \\ 0 & 0 & \alpha_f \alpha_g \rho_g + \rho_{AP} & -(\alpha_g \alpha_f \rho_f + \rho_{AP}) \end{pmatrix} \tag{17}$$

$$B=\begin{pmatrix} \dfrac{\alpha_g v_g}{a_g^2} & \rho_g v_g & \alpha_g\rho_g & 0 \\ \dfrac{\alpha_f v_f}{a_f^2} & -\rho_f v_f & 0 & \alpha_f\rho_f \\ 1 & \beta_g-\beta_f & \alpha_g\rho_g v_g & \alpha_f\rho_f v_f \\ 0 & \alpha_f\beta_g+\alpha_g\beta_f & \begin{matrix}\left[\alpha_f\rho_g+\rho_f C_{vm}(\lambda-1)\right]v_g \\ -\rho_f C_{vm}(\lambda-2)v_f\end{matrix} & \begin{matrix}-\left[\alpha_f\rho_f+\rho_f C_{vm}(1-\lambda)\right]v_f \\ -\rho_f C_{vm} v_g\lambda\end{matrix} \end{pmatrix} \tag{18}$$

Recognizing that the phase velocities are much smaller than the phasic sounds speeds, that is, $a_g^2 >> v_g$ and $a_f^2 >> v_f$, the characteristic polynomial is then given by the determinant,

$$\begin{vmatrix} 0 & \rho_g(\mu-v_g) & -\alpha_g\rho_g & 0 \\ 0 & -\rho_f(\mu-v_f) & 0 & -\alpha_f\rho_f \\ -1 & \beta_f-\beta_g & \alpha_g\rho_g(\mu-v_g) & \alpha_f\rho_f(\mu-v_f) \\ 0 & -(\alpha_f\beta_g+\alpha_g\beta_f) & \begin{Bmatrix}\alpha_f\rho_g+\rho_f C_{vm}\ (\mu-v_g) \\ -\rho_f C_{vm}(\lambda-2)(v_g-v_f)\end{Bmatrix} & \begin{Bmatrix}-\ \alpha_f\rho_f+\rho_f C_{vm}\ (\mu-v_f) \\ +\rho_f C_{vm}\lambda(v_g-v_f)\end{Bmatrix} \end{vmatrix}=0 \tag{19}$$

which can be shown to be equivalent to the following second degree polynomial in μ:

$$\begin{vmatrix} \rho_g(\mu-v_g) & -\alpha_g\rho_g & 0 \\ -\rho_f(\mu-v_f) & 0 & -\alpha_f\rho_f \\ -(\alpha_f\beta_g+\alpha_g\beta_f) & \begin{Bmatrix}\alpha_f\rho_g+\rho_f C_{vm}\ (\mu-v_g) \\ -\rho_f C_{vm}(\lambda-2)(v_g-v_f)\end{Bmatrix} & \begin{Bmatrix}-\ \alpha_f\rho_f+\rho_f C_{vm}\ (\mu-v_f) \\ +\rho_f C_{vm}\lambda(v_g-v_f)\end{Bmatrix} \end{vmatrix}=0 \tag{20}$$

To simplify the algebra, the following transformations will be applied:

$$\begin{aligned} v_r &= v_g - v_f \\ A &= \rho_f C_{vm} \\ B &= -(\alpha_f\beta_g+\alpha_g\beta_f) \\ r &= \lambda - v_g \end{aligned} \tag{21}$$

With the above transformations, the quadratic corresponding to Equation (20) is of the form,

$$ar^2+br+c=0 \tag{22}$$

where,

$$\begin{aligned} a &= \alpha_f{}^2\rho_g + \alpha_g\alpha_f\rho_f + A \\ b &= \left[A(2-\lambda) + 2\alpha_g\alpha_f\rho_f\right]v_r \\ c &= \alpha_g\alpha_f(\rho_f v_r{}^2 + B) + \alpha_g A(1-\lambda)v_r{}^2 \end{aligned} \tag{23}$$

It has been shown [4] that the best fit to measurements of sounds speed are obtained when $\lambda \to 2$. This is true for measurements of sound speed in air-water as well as steam-water (at ~ 0.267 MPa, 402 K).

Also, for mixed flow regime, the phase to interphase pressure differences is given by,

$$\beta_k = C_p\rho_m v_r{}^2 \tag{24}$$

where $\rho_m = \alpha_g\rho_g + \alpha_f\rho_f$ is the mixture density and $k = f, g$ and C_P is a multiplier to be determined. In what follows, it will be shown that selection of C_P must be made with care to avoid complex characteristics. It is easy to show that $B = -(\alpha_f\beta_g + \alpha_g\beta_f) = -C_p\rho_m v_r{}^2$. Thus, the coefficients of the quadratic in Equation (22) can be shown to be given by,

$$\begin{aligned} a &= \alpha_f{}^2\rho_g + \alpha_g\alpha_f\rho_f + A \\ b &= 2\alpha_g\alpha_f\rho_f v_r \\ c &= \left[\alpha_g\alpha_f(\rho_f - \rho_m C_p) - \alpha_g A\right]v_r{}^2 \end{aligned} \tag{25}$$

For real eigenvalues, the discriminant of the quadratic in Equation (22) must be positive. Thus, we have the condition:

$$\rho_f{}^2 C_{vm}{}^2 + \alpha_f\rho_f C_{vm}(\rho^* + C_p\rho_m - \rho_f) + \alpha_f{}^2(\alpha_g\rho_f{}^2 - \rho_f\rho^* + C_p\rho^*\rho_m) > 0 \tag{26}$$

where

$$\rho^* = \alpha_g\rho_f + \alpha_f\rho_g \tag{27}$$

The apparent mass coefficient, C_{vm} and the coefficient of phase-to-interface pressure term, C_p, must be selected in such a way that inequality (26) must be satisfied for all fluid states. Possible range of values for C_{vm} and C_P are discussed for all possible cases below.

3.1 No virtual mass or phase-to-interphase pressure difference terms

If $C_{vm} = C_p = 0$, both the virtual mass and interface pressure terms will vanish. In this case, inequality (26) can be shown to reduce to:

$$\alpha_g > \alpha_g + \alpha_f \frac{\rho_g}{\rho_f} \tag{28}$$

Clearly, this condition can never be satisfied. As a result, for this case, the equations are always ill-posed (complex characteristics).

3.2 Non-zero phase-to-interphase pressure difference terms

If $C_{vm} = 0$ and $C_p \neq 0$, then, for real characteristics C_p must be chosen such that,

$$C_p > \left[1 - \alpha_g \left(1 - \frac{\rho_g}{\rho_f}\right)\right]^{-1} \left(1 - \alpha_g \left\{1 + \alpha_g \left(1 - \frac{\rho_g}{\rho_f}\right)\right\}^{-1}\right) \tag{29}$$

In Figure 1 the lower bound to Equation (29) has been plotted for pressures ranging between 0.1 MPa to 10 MPa. It is observed that in the absence of virtual mass term, interface-to-phase pressure terms can still render the equations well-posed as long as C_p remains above the curve corresponding to 10 MPa (assuming a typical CANDU simulation). In implementation, the inequality sign in Equation (29) would have to replaced with the equality sign. The current value used in CATHENA 3 is $C_p = 0.17$.

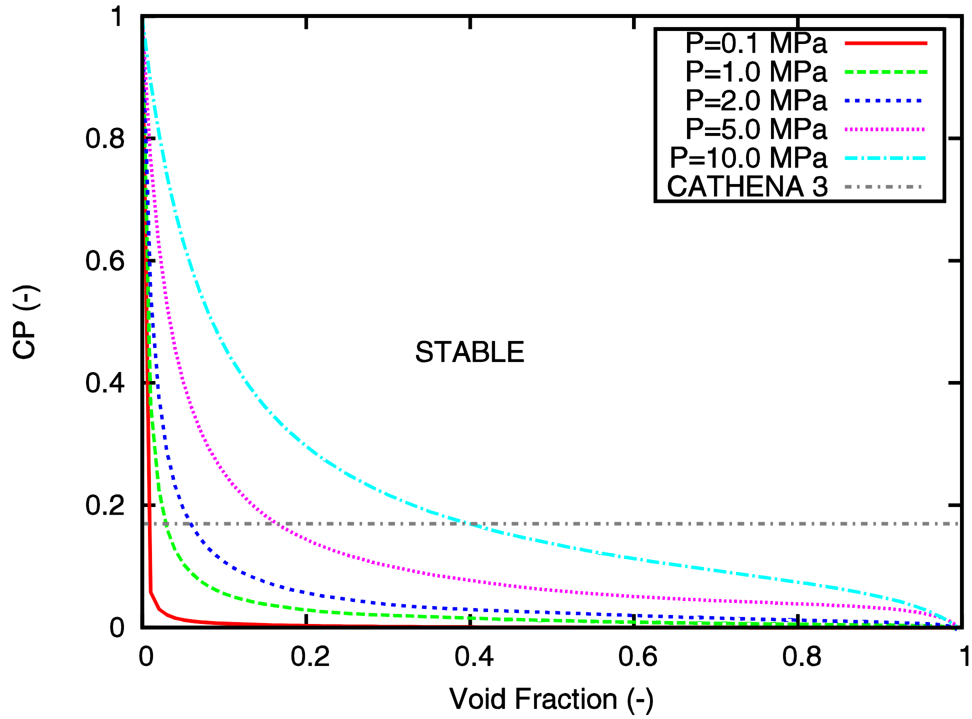

Figure 1 Phase-to-interface pressure multiplier for $C_{vm} = 0$ from Eqn. (29).

3.3 Non-zero virtual mass coefficient

If $C_p = 0$ and $C_{vm} \neq 0$, then, for real characteristics C_{vm} must be chosen such that,

$$C_{vm} = \frac{1}{2}\alpha_f{}^2\left(1-\frac{\rho_g}{\rho_f}\right)+\frac{1}{2}\left\{\alpha_f{}^3\left[\alpha_f(1-\frac{\rho_g}{\rho_f})^2+4\frac{\rho_g}{\rho_f}\right]\right\}^{1/2} \tag{30}$$

which is a lower bound since the inequality has been replaced by the equality sign. In Figure 2 Equation (30) has been plotted for pressures ranging between 0.1 MPa to 10 MPa. It is observed that in the absence of the interface-to-phase pressure terms, the equations can still be rendered well-posed for a wide range of pressures if C_{vm} is chosen such that it remains above the values determined from Equation (30). It is noted that the dependence of this equation on the density ratio is very weak. Taking advantage of this property, if the density ratio in Equation (30) is set to zero, the following simple relation is obtained for the lower bound virtual mass coefficient:

$$C_{vm} = (1-\alpha_g)^2 \tag{31}$$

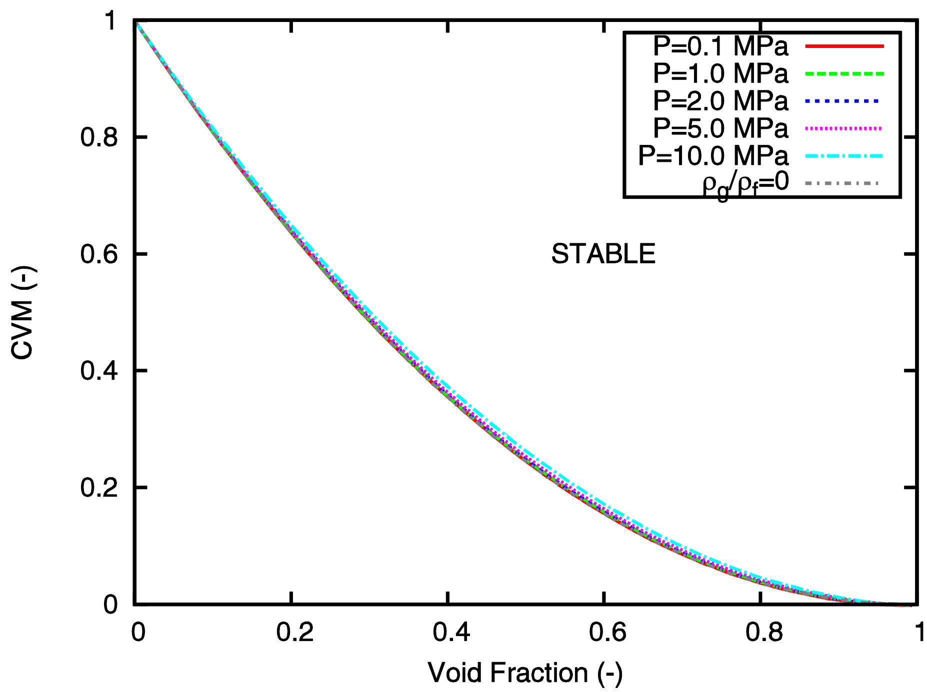

Figure 2 Virtual mass coefficient for $C_p = 0$ from Eqn. (30) and (31).

Equation (31) is also plotted in Figure 2; as expected it is indistinguishable from the plots given by the more general expression given in Equation(30). This is remarkable and it suggests that the equations can be rendered well-posed if the coefficient of virtual mass is given by Equation (31) for the case $\lambda = 2$ in Drew's objective form for the virtual mass, given in Equation (4).

3.4 Non-zero virtual mass and phase-to-interface pressure difference terms

The most general case is when $C_{vm} \neq 0$ and $C_p \neq 0$. Under these conditions, using the inequality in Equation (26) it can be shown that the virtual mass coefficient, C_{vm}, is given by,

$$C_{vm} > \frac{1}{2}\alpha_f\left[\alpha_f(1-\frac{\rho_g}{\rho_f}) - C_p\frac{\rho_m}{\rho_f}\right] + \frac{1}{2}\alpha_f\left\{\left[\alpha_f(1-\frac{\rho_g}{\rho_f}) - C_p\frac{\rho_m}{\rho_f}\right]^2 - 4\left[C_p\left(1-\alpha_f(1-\frac{\rho_g}{\rho_f})\right)\left(\alpha_f(1-\frac{\rho_g}{\rho_f}) + \frac{\rho_g}{\rho_f}\right) - \alpha_f\frac{\rho_g}{\rho_f}\right]\right\}^{\frac{1}{2}} \tag{32}$$

Since the ratio $\frac{\rho_m}{\rho_f}$ can be shown to be equal to $\alpha_g\frac{\rho_g}{\rho_f} + \alpha_f$, it is observed that C_{vm} is a function of void fraction and the density ratio (or pressure) only.

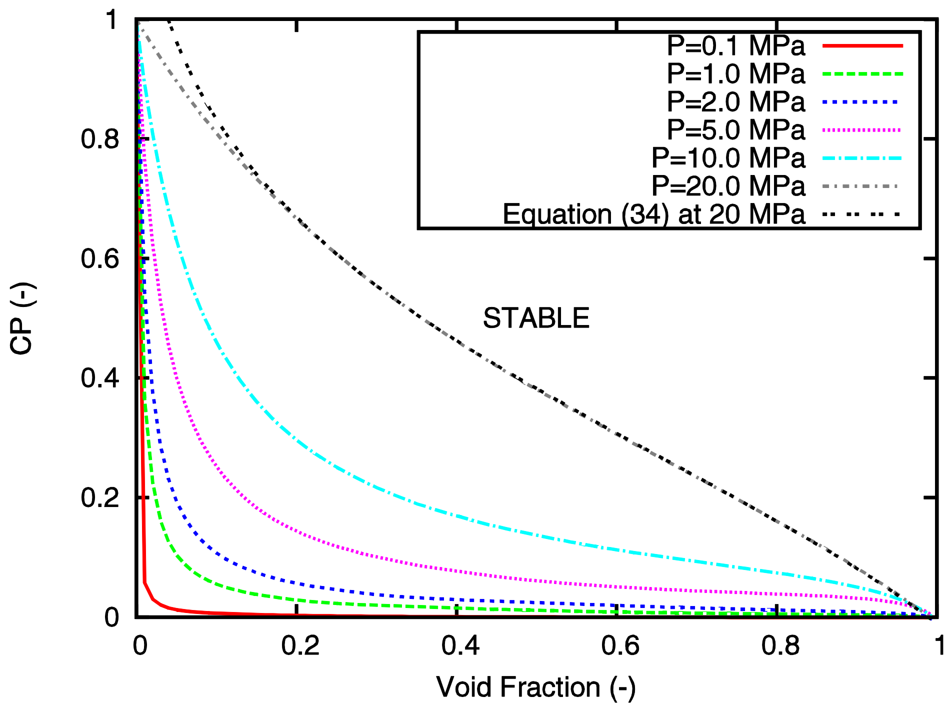

Figure 3 Phase-to-interface pressure multiplier from Eqn. (34).

Equation (32) provides the most general form for the virtual mass coefficient but it must be noted that at this point, C_p still is indeterminate. The restrictions imposed on C_p can easily be stated since complex as well as negative values for C_{vm} must be excluded. Thus, the portion of Equation (32) that is under the square root must be non-negative. This imposes the following condition on the phase-to-interface pressure coefficient, C_p:

$$\left[\alpha_f(1-\frac{\rho_g}{\rho_f}) - C_p\frac{\rho_m}{\rho_f}\right]^2 - 4\left[C_p\frac{\rho^*}{\rho_f}\frac{\rho_m}{\rho_f} - \alpha_f\frac{\rho_g}{\rho_f}\right] > 0 \tag{33}$$

Solving for C_p and replacing α_f with $1-\alpha_g$, the following relation is obtained,

$$C_p > 2\left(\frac{1-\frac{1}{2}(1-\alpha_g)(1-\frac{\rho_g}{\rho_f})-\sqrt{\alpha_g}}{1-\alpha_g(1-\frac{\rho_g}{\rho_f})}\right) \tag{34}$$

Equation (34) gives the lower bound on C_p which is consistent with the definition of C_{vm}. Equation (34) is plotted at 20 MPa in Figure 3, showing its relation to the limiting cases that were presented earlier in Figure 1. The plotting range has been extended to cover up to 20 MPa to provide guidance for code developers who work on supercritical water reactor applications. It is observed that the form of C_p that is consistent with the definition of C_{vm} is the curve that bounds all other curves. Therefore, if a formulation of two-phase flow where both virtual mass and phase-to-interface pressure terms are present is used, Equation (34) provides a limiting envelope and all formulations of C_p must lie above this curve. In implementation, the developers are advised to use Equation (34) in its equality form which will then provide for a formulation dependent on density ratio (i.e. pressure) and void fraction.

Substituting C_p given in Equation (34) in Equation (32) and taking the lower bounding curve (that is, changing the '>' operator to '=' operator), the most general form of the virtual mass coefficient which satisfies Drew's objectivity condition can be obtained:

$$C_{vm} = \frac{1}{2}(1-\alpha_g)\left\{(1-\alpha_g)(1-\frac{\rho_g}{\rho_f})-\left[\left(1+\frac{\rho_g}{\rho_f}+\alpha_g(1-\frac{\rho_g}{\rho_f})\right)-2\sqrt{\alpha_g}\right]\right\} \tag{35}$$

Equation (35) is plotted in Figure 4 for various pressures, up to supercritical conditions.

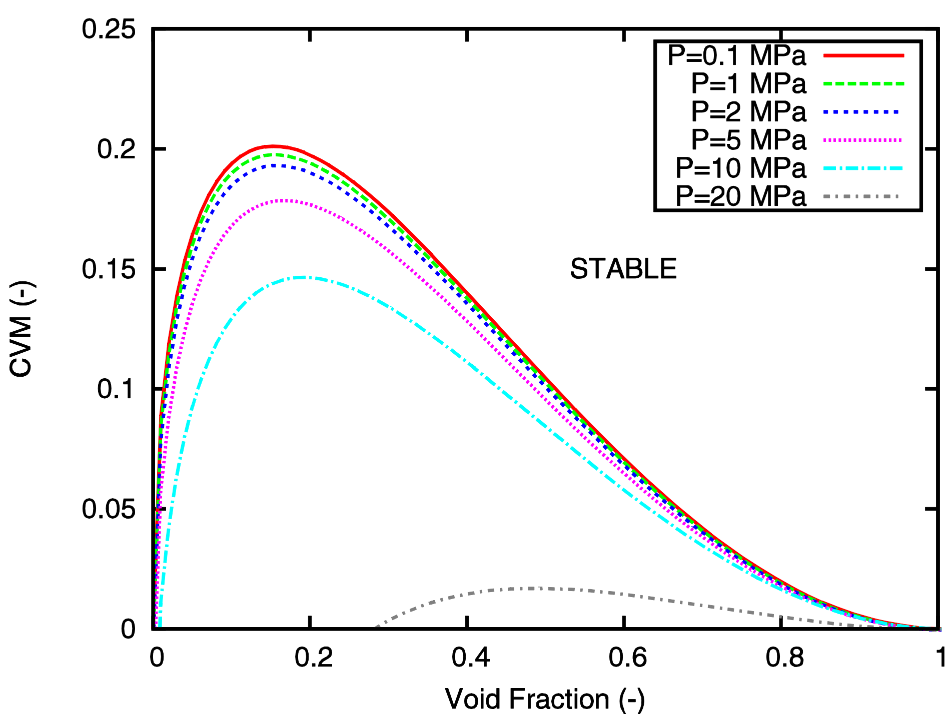

Figure 4 Virtual mass coefficient from Eqn. (35).

It is observed that the restriction on C_{vm} becomes tighter as pressure decreases. In application, is it recommended that Equation (35) is implemented and the density ratio is kept as one of the model parameters. It is also observed that in the presence of phase-to-interface pressure difference terms, virtual mass coefficient can take lower values (compare with Figure 2) and still render the system of equations hyperbolic. The only condition is that the coefficient of phase-to-interface pressure difference, C_p must obey the inequality (34). In implementation, this inequality must be converted to an equality, providing the lower bound for C_p. Equation (35) can then be used to ensure that the two models do not interfere with each other as far as the hyperbolicity of the partial differential equations is concerned.

4. Conclusion

An important conclusion of the present analysis is that, models for virtual mass coefficient and the phase-to-interface pressure difference coefficients may not be specified independently. Drew's law of objectivity given in Equation (4) leads to the most general form of C_{vm} given in Equation (32) as a function of C_p. However, this form places its own restrictions on C_p, which leads to the only admissible form of C_p given in Equation (34). It turns out that this form of C_p is also the curve that bounds all cases that were obtained for the simple case $C_{vm} = 0$. The most general formulation of C_{vm} consistent with the formulation of phase-to-interface pressure difference terms is given in Equation (35). As part of future work, the implications of the present analysis should be investigated on the discretised form of the governing equations.

5. References

[1] B.N. Hanna, "CATHENA: A Thermalhydraulic Code for CANDU Analysis", *Nuclear Engineering and Design*, 180, 1998, pp.113-131.

[2] N.U. Aydemir and B.N. Hanna, "CATHENA 4: A Thermalhydraulic Network Analysis Code", The 13th International Topical Meeting on Nuclear Reactor Thermal Hydraulics (NURETH-13), Kanazawa City, Ishikawa Prefecture, Japan, 2009, Sep 28-Oct 2.

[3] D. Drew, L. Cheng and R.T. Lahey, "The Analysis of Virtual Mass Effects in Two-Phase Flow", *Int. J. Multiphase Flow*, 5, 1979, pp. 233-242.

[4] T. Watanabe, M. Hirano and F. Tanabe, "The Effect of Virtual Mass Term on The Stability of Transient Two-Phase Flow Analysis", JAERI-M89-101, Japan Atomic Energy Research Institute, 1989, Japan.

[5] T. Watanabe and Y. Kukita, "The Effect of Virtual Mass Term on the Two-Fluid Model Against Perturbations", *Nuclear Engineering and Design*, 135, 1992, pp.327-340.

[6] J.H. Stuhmiller, "The Influence of Interfacial Pressure Forces on the Character of Two-Phase Flow Equations", *Int. J. Multiphase Flow*, 3, 1977, pp. 551-560.